Materials Today Bio 29 (2024) 101262

Contents lists available at ScienceDirect

Materials Today Bio

journal homepage: www.journals.elsevier.com/materials-today-bio

Personalized PDAC chip with functional endothelial barrier for tumour biomarker detection: A platform for precision medicine applications

Karina Goluba [a,1], Vadims Parfejevs [a,1], Evita Rostoka [a], Kaspars Jekabsons [a], Ilze Blake [a], Anastasija Neimane [a], Annija Anete Ule [b], Roberts Rimsa [b], Reinis Vangravs [c], Andrejs Pcolkins [d], Una Riekstina [a,*]

[a] Pharmaceutical Sciences Center, Faculty of Medicine and Life Sciences, University of Latvia, Jelgavas iela 3, Riga, Latvia
[b] Institute of Solid State Physics, University of Latvia, Kengaraga iela 8, Riga, Latvia
[c] Latvian Centre of Infectious Diseases, Laboratory Service, Riga East University Hospital, Linezera iela 3, LV-1006, Riga, Latvia
[d] Department of Abdominal and Soft Tissue Surgery, Riga East Clinical University Hospital, Hipokrata iela 2, Riga, Latvia

A B S T R A C T

Pancreatic ductal adenocarcinoma (PDAC) is a highly aggressive cancer characterised by poor survival rates and an increasing global incidence. Advances in the staging and categorization of pancreatic tumours, along with the discovery of functional mutations, have made precision treatments possible, which may lead to better clinical results. To further improve customized treatment approaches, in vitro models that can be used for functional drug sensitivity testing and precisely mimic the disease at the organ level are required. In this study, we present a workflow for creating a personalized PDAC chip utilising primary tumour-derived human pancreatic organoids (hPOs) and Human Umbilical Vein Endothelial Cells (HUVECs) to simulate the vascular barrier and tumour interactions within a PDMS-free organ-on-a-chip system. The patient PDAC tissue, expanded as tumour hPOs, could be cultured as adherent cells on the chip for more than 50 days, allowing continuous monitoring of cell viability through outflows from tumour and endothelial channels. Our findings demonstrate a gradual increase in cell density and cell turnover in the pancreatic tumor channel. Tumour-specific biomarkers, including CA-19.9, TIMP-1, Osteopontin, MIC-1, ICAM-1 and sAXL were consistently detected in the PDAC chip outflows. Comparative analyses between tissue culture plates and microfluidic conditions revealed significant differences in biomarker secretion patterns, highlighting the advantages of the microfluidics approach. This PDAC chip provides a stable, reproducible tumour model system with a functional endothelial cell barrier, suitable for drug sensitivity and secretory biomarker studies, thus serving as a platform for functional precision medicine application and multi-organ chip development.

1. Introduction

Pancreatic ductal adenocarcinoma (PDAC) is a prevalent form of pancreatic cancer, comprising about 80 % of the cases [1]. PDAC is one of the most aggressive cancers commonly diagnosed in an advanced stage, resulting in ~10 % overall survival beyond 5 years for patients with all forms of PDAC and a dismal 3 % for patients with metastatic disease [2]. Considering the general ageing of society, obesity, the epidemic of type 2 diabetes and other factors that contribute to the development of pancreatic cancer [3,4], PDAC incidence and PDAC-related deaths are expected to double in the next ten years [5,6]. Along with the advancements in treatment options, identifying relevant biomarkers and refining early detection methods is crucial for improving patient survival [7]. In fact, cumulative efforts over the last decade have led to the two-fold improvement of survival statistics and hold promise for the future [8].

Molecular profiling has broadened the understanding of the genetic and transcriptional PDAC landscape. Aberrations in *KRAS* are the most frequent among PDAC patients with more than 90% prevalence and appear early in the precursor lesion stage. These are often followed by changes in *CDKNA2* pertaining to low-grade disease and *TP53* and *SMAD4*, which are associated with high-grade PDAC. Other mutations found with less than 10% frequency include changes in DNA repair (*BRCA1*, *BRCA2*) and chromatin remodelling associated genes (*ARID1A*, *KDM6A*), as well as alternative driver mutations (e.g *BRAF*) [8]. Based on the molecular features, PDAC has been divided into classical and basal-like subtypes [9]. The basal PDAC subtype is being associated with a less favourable chemotherapy treatment outcome [10].

In addition to improved standard chemotherapy, personalized targeted PDAC therapy is evolving, with treatment decisions depending on

* Corresponding author.
E-mail address: una.riekstina@lu.lv (U. Riekstina).
[1] These authors contributed equally.

https://doi.org/10.1016/j.mtbio.2024.101262
Received 2 July 2024; Received in revised form 7 September 2024; Accepted 20 September 2024
Available online 21 September 2024

the type of genetic alterations in tumour cells [11,12]. However, the sensitivity of the neoplastic cells to chemotherapy is also regulated by elements that are more difficult to account for, such as tumour microenvironment (TME) and epigenetic determinants [11]. In the case of highly desmoplastic PDAC, where cancerous cells can be a minority, TME plays a crucial role and could be equally responsible for tumour aggressiveness and resistance to the treatment [8]. Indeed, there is a complex interplay between neoplastic and TME components as well as the physical barrier factor that contribute to chemoresistance [13–15]. To further advance treatment outcomes, functional precision medicine approaches combining drug sensitivity tests with genomic analysis have been suggested for tumours that are difficult to treat [16].

Several platforms have been considered for drug sensitivity tests in precision medicine. The organoid culture approach complements studies performed in cancer cell lines and animal models [17]. These self-organising 3D cellular structures provide improved recapitulation of structural and functional properties of the original tissue. Recent protocols have allowed deriving both normal and tumour organoid cultures of the exocrine pancreas from human primary tissue [18,19]. Organoid technology enables in-depth analysis of pancreatic cancer subtypes [20] and drug screens [19]. Organoid-based platforms have been successfully used in personalized medicine approaches for novel drug discovery and to predict the efficiency of chemotherapy in PDAC [21].

Similarly, many efforts have been directed at the development of the advanced PDAC 3D models to better mimic the tumour microenvironment. Bioengineering techniques such as two-photon polymerization, hybrid scaffold designs, and novel hydrogels are employed to recreate in vivo-like tumour structures. For example, 3D-printed microscale scaffolds with bioactive coatings (e.g., hyaluronic acid, fibronectin) have been used to study early-stage metastasis [22]. Ex vivo explant models preserve the original tumour architecture for direct therapeutic testing on PDAC patient tissue [23]. Other studies explore biocompatible scaffolds like polyvinyl alcohol/gelatin to support cancer cell growth and tumour aggressiveness [24]. Long-term tri-culture models with hybrid polyurethane scaffolds mimic key PDAC features, such as desmoplasia, for over five weeks [25]. Innovative hydrogels promote spheroid formation for studying tumour invasiveness markers [26], while the cancer-on-a-bead model replicates the tumour microenvironment, emphasizing the role of the extracellular matrix in drug resistance [27].

Nevertheless, several aspects of the tumor environment and drug delivery remain challenging to replicate in both 2D models and more advanced 3D and organoid cultures. The delivery of the chemical agent to the tumour cells is influenced by both the characteristics and behaviour of the chemical preparation in the blood flow, as well as the properties of the components of the bloodstream, such as plasma pharmacokinetics, tumour vessel structure, including endothelial permeability, vessel diameter and branching [28,29]. Models that could consider these dimensions and simulate how much of the chemical agent passes from the flow in the blood vessel to the tumour cells would be beneficial.

In recent years, microfluidic devices allowing long-term co-culture of different cell types and simulation of physiological barrier function, often termed organs-on-the-chip (OOC) have become increasingly popular [30]. By adding the possibility to modulate dynamic mechanical signals on the cells (e.g. fluid shear stress, interstitial fluid flow, waste removal etc.) [31] or spatiotemporal chemical gradients [32], it is possible to bring the in vitro microfluidic system closer to the organ or tumour of interest [30,33].

Various PDAC-on-the-chip approaches have been proposed exploring tumour cell cross-talk with stromal components [34–37] and vascular endothelium [38]. A trend to incorporate primary cells in microfluidic devices is noticeable and often preferred for more accurate effect modelling [30]. Several recent studies used donor tissue-derived PDAC organoids [34,36] or tumour spheroids [39] embedded in the ECM gel. However, the concept of harnessing primary PDAC tissue in the chip with a focus on endothelial/epithelial barrier allowing flow manipulation has not been explored so far.

Here, we partially integrate previous approaches and describe a workflow for generating personalized PDAC-on-the-chip (PDAC chip) that brings primary tumour tissue expanded as organoids in direct contact with the blood vessel barrier. The system allows long-term co-culture with repeated readouts and offers control of the media flow rate. First, we produce a vertically stacked-channel polydimethylsiloxane (PDMS)-free microfluidic chip that simulates blood vessel and pancreatic duct lumens, separated by a porous membrane and providing separate outflow collection. We characterise the microfluidic system and compare it to a 2D culture model. Such microfluidic device could be used to simulate and manipulate blood flow and permeability parameters, to study PDAC/vasculature interaction and to clarify the pharmacokinetics, pharmacodynamics and efficacy of the chemical agents. We demonstrate that reliable biomarker readouts can be obtained specifically from the chip samples aided by PDMS-free chip and experimental setup. These readouts could be useful to monitor the system, assess drug sensitivity and could be integrated into personalized functional oncology approaches to predict therapy response.

2. Material and methods

2.1. Primary human pancreatic tumour organoid derivation and culture

Primary human pancreatic organoids (hPOs) were derived from donor tumour tissue following the pancreatic ductal adenocarcinoma (PDAC) resection procedure performed in Riga East Clinical University Hospital. The study was approved by the Central Medical Ethics Committee of Latvia (approval Nr. 7028 from July 21, 2021) and patient informed consent was obtained. Tissue samples were transferred in transportation solution Ad-DMEM+++ containing Ad.DMEM/F12 (Gibco, #12634010) 2 mM GlutaMAX Supplement (Gibco, #35050061), 10 mM HEPES (Gibco, #15630080), 100 units/ml Pen/Strep (Sigma-Aldrich, #P4333) and isolated within 24 h. Pancreatic organoids were established following a previously published protocol [40]. The tissue samples were minced into smaller fragments using scissors, a portion was collected for DNA and RNA isolation and placed at −80°C freezer for later isolation. The minced tissue was transferred to a 15 ml tube and washed three times with D-BSA, containing DMEM (Sigma-Aldrich, #D0822) and 0.1% BSA (Sigma-Aldrich, #SLCK4304) on ice. Each washing step included sample pipetting, allowing minced tissue to sediment and removal of the supernatant. The sample was enzymatically digested in a solution, containing Ad-DMEM+++, 1 mg/ml Collagenase type II (Gibco, #17101015), 100 μg/ml Trypsin inhibitor (Gibco, #R007100) and 10 μM rock inhibitor (Y27632) (AbMole BioScience, #M1817). Digestion was carried out in a 37° C incubator with a shaker at 140 rpm for 2 h and included a pipetting step every 30 min with a pre-wetted 5 ml serological pipette. The digestion process was stopped by adding 1 ml FBS (Gibco, #16141079). The sample was washed with D-BSA and filtered over a 100 μm pore size filter in a 50 ml tube. The collected flow-through was centrifuged in a 15 ml plastic tube and centrifuged at 1200 RPM for 5 min. The pellet was placed on ice and resuspended in Culturex BME Type II gel (R&D Systems, #3533-005-02). 50 μl of gel was used to make four individual domes per well in a 24-well low-adhesion pre-heated plate (Sarstedt). The plate was inverted and placed in the incubator at 37°C, 5 % CO_2 for 20 min allowing the gel to solidify. After 20 min 0.5 ml of organoid full medium containing AdDMEM/F12, 10,000 units/mL Pen/Strep, 40 % Wnt3A conditioned medium, 2 mM Glutamax, 10 mM Hepes, 1x B27 supplement (Gibco, #17504044), 1x N2 supplement (Gibco, #17502048), 1.25 mM N-acetylcystein (Sigma-Aldrich, #A7250), 10 mM Nicotinamide (Sigma-Aldrich, #240206), 10 nM Gastrin (Sigma-Aldrich, #G9145), 10 % RSPO conditioned medium (homemade), 50 ng/ml Noggin (Peprotech, #120-10C), 100 ng/ml FGF10 (Peprotech, #100-26), 50 ng/ml EGF, 1 μM Forskolin (Tocris, #1099), 0.5 μM A83-01 (Tocris, #2939), 50 μg/ml Primocin (InvivoGen, #ant-pm-2),

10 ng/ml FGF2 (Peprotech #100-18B) and Y27632 was added to wells and plate was placed back in the incubator.

2.2. Human umbilical vein endothelial cell culture

Human Umbilical Vein Endothelial Cells (HUVEC) (#SCCE001, Millipore Chemicon®) were cultured in a T75 flask in EndoGRO-VEGF Complete Culture Media Kit (cat. nr. SCME002, Millipore) medium, based on the manufacturer's instructions. Cells up to passage 7 were used in the experiments.

2.3. DNA isolation and targeted sequencing

DNA was isolated from tumour hPOs after reaching passage five. Tumour hPOs were mechanically isolated from the gel by washing and pelleted. Isolation was performed using a QIAamp® DNA Mini kit (Qiagen, #157055028) according to the manufacturer's instructions. The sequencing libraries were prepared with the QIAseq Targeted DNA Human Comprehensive Cancer Panel DHS-3501Z (Qiagen, Germany) following the manufacturer's protocol. The panel included 11,311 primers targeting regions in genes, with a total length of 836.7 kilobases. The libraries were quantified via qPCR and size-estimated with TapeStation (Agilent, USA) before equimolar pooling for sequencing.

The pooled libraries were sequenced on the Illumina NextSeq 550dx platform using the High Output reagent kit in 150 PE configuration, producing approximately 60 million paired reads per sample. Data processing and variant calling were conducted with Qiagen CLC Genomics Workbench (v23.0.1), using the default workflow from the Biomedical Genomics Analysis module (v23.0.1) and the GRCh37 reference genome. Interpretation of the obtained variants was performed using Qiagen Clinical Insight software.

2.4. Microfluidic chip fabrication

Off-stoichiometry thiol-ene (OSTE)/cyclo-olefin copolymer (COC) devices were based on COC mini-luer port microscope slides (Microfluidic ChipShop, Germany) for the top channels and COC microscope slides (Microfluidic ChipShop, Germany) for the bottom pieces. The chips have a vertically stacked design with a channel height of 1.25 mm for the top channel (used for epithelial cells) and 0.20 mm for the bottom channel (utilized for endothelial cells), with an overlapping area of 18 mm^2, with 1.2 and 1.0 mm channel widths, respectively. The chip initially was designed in 3D CAD software Solidworks (DS Solidworks Corp., USA) The master molds for OOC channel fabrication were then 3D printed with a masked stereolithography (MSLA) 3D printer (Zortrax Inkspire, Zortrax, Poland) with ivory resin. The prepared master mold was then washed in an ultrasonic bath for 10 min in isopropyl alcohol and blow-dried using N2 followed by UV (6.6 mW/cm^2 for 30 min) and thermal treatment (60°C for 48 h) to fully cure the master mold. Then PDMS was mixed in a 10:1 ratio and cured in the molds at 60°C overnight. Cured PDMS was peeled off a 3D-printed mold, using isopropyl alcohol for wetting and easier peeling.

For device fabrication A and B components of OSTE 322 (Mercene labs, Sweden) were mixed in w/w proportion 1.09:1, as per manufacturer's instructions, followed by mixing in Mixer Thinky with 750 rpm for 5 min in the mixing program and 750 rpm for 5 min in the defoaming program. Mixed OSTE was degassed using a vacuum desiccator for ~20 min. COC slide's surfaces were oxidized using Plasma Asher (GIGAbatch 360 M, PVA Tepla, USA) with a flow rate of 800 sccm (O_2), power 600 W for 2 min. To prepare the bottom layer of the chip, the PDMS mold was pressed against the COC slide in a jig, and a glass slide on top was secured tightly with 6 M4 screws (at 0.3 Nm). OSTE container was connected to the PDMS mold using polytetrafluoroethylene (PTFE) tubing, and OSTE injection was done using Microfluidic Flow Controller OB1 MK3+ (Elveflow, France). Injected OSTE was exposed in UV using Mask Aligner Suss MA6 with a dose of 850 mJ. The COC slide with exposed OSTE was peeled of the jig and pressed against a 20 μm thick porous polyethylene terephthalate (PET) membrane (3 μm pore size, 0.8E6 pores/cm^2, porosity of 5.65%, (it4IP, Belgium) so that air bubbles are pressed out. The COC/OSTE bottom layer was cured on a hot plate at 60°C for 1 h between PTFE films with 2 kg weight pressing the devices to the hot-plate. To prepare the top layer, OSTE injection was done the same way as for the bottom layer and exposed to UV with a dose of 925 mJ. Finally, the top and bottom layers were aligned using an adapted alignment tool and pressed together, pressing out any air pockets. OSTE/COC hybrid device was compressed from both sides using a custom setup and left to cure in an oven at 60°C overnight. Internal process control for chips included alignment control to ensure consistency for the cell culture area, and bottom channel fluidic resistance testing. Resistance testing was done at 50 mbar pressure with 10% (v/v) isopropyl alcohol and de-ionised water mixture for every channel, which allowed us to obtain the volume flow rate through every channel. The resistance testing allowed to control for constant bottom channel height, which otherwise cannot be tested non-destructively. Given the fact that for square channel profiles, the flow resistance is impacted by channel height to the power of 3 [41], it was possible to control that the channel height varies no more than ± 10 % from the 0.2 mm design. The overall chip dimensions are that of a standard microscopy slide of 75.5 x 25.5 mm. Fig. 1 shows the chip setup scheme.

2.5. HUVEC and tumour hPO seeding on the chip

The microfluidic chip was rinsed with 70% ethanol and dH2O at a flow rate of 10 μl/min for 2 h and 4 μl/min for up to 4h. The chip membrane was coated with Cultrex BME Type II gel at a ratio of 1:100 (0.1 mg/ml) in Advanced DMEM/F12 (#12634010, GibcoTM) before cell seeding. Initially, the bottom channel of the chip was coated with 50 μl of the coating solution, the output and input ports were closed with mini luer plugs (ChipShop, #10000053) and the chip was placed in an incubator 37°C, 5% CO_2 for 30 min, upside down, to allow coating to adhere to the membrane. In the meantime, HUVECs were trypsinised according to manufacturer instructions and counted using LUNA II cell counter (Logos Biosystems). Channels were seeded at 6x10e6 cells/ml concentration using 50 μl cell suspension per channel, inverted and placed in a 37°C, 5% CO2 incubator for 2 h for cell attachment to the membrane. After 2 h the chip was removed from the incubator and connected to the syringe pump ISPLab10 (DK Infusetek) using HUVEC medium at 4 μl/min flow rate and cultured until endothelial cells were fully confluent. Syringes with the cell culture media were connected to the chip inlets via Teflon tubing, while the outlets were connected to the media-collecting sample tubes placed in the incubator along the chip. A similar seeding procedure was used for tumour hPOs, except the flow to the lower channel was stopped prior upper channel coating and cell seeding process.

Tumour hPOs were dissociated to a single cell level by adding 0.5 ml Collagenase/Dispase solution (Roche #10269638001) in AD/DMEM+++ containing 10 μM Y27632 to a phosphate buffered saline (PBS)-rinsed well (24-well plate), and incubating at 37°C 5% CO2 for 2 h. After digestion tumour hPOs were washed with D-BSA and further digested using 0.5 ml Accutase (Gibco, #A1110501) with 10 μM Y27632 in a water bath at 37°C for 40 min, pipetting cell pellet every 15 min and checking for cell dissociation. Digestion was stopped with Ad-DMEM+++ solution, cells were centrifuged for 5 min at 1200 rpm and resuspended in full tumour hPO medium with 10 μM Y27632. Cells were seeded on the chip using one full tumour hPO well (24-well plate) per chip channel and placed in the incubator for 3 h for attachment in 50 μl of full hPO medium with 10 μM Y27632. After 3 h the chip was removed from the incubator, upper channels were connected to the syringe system using tumour hPO full medium diluted with AD/DMEM+++ in 1:5 ratio (adjusted to 50 ng/ml EGF, 10 mM Nicotinamide and 1.25 mM N-acetylcysteine) concentrations and set to flow rate of 4 μl/min.

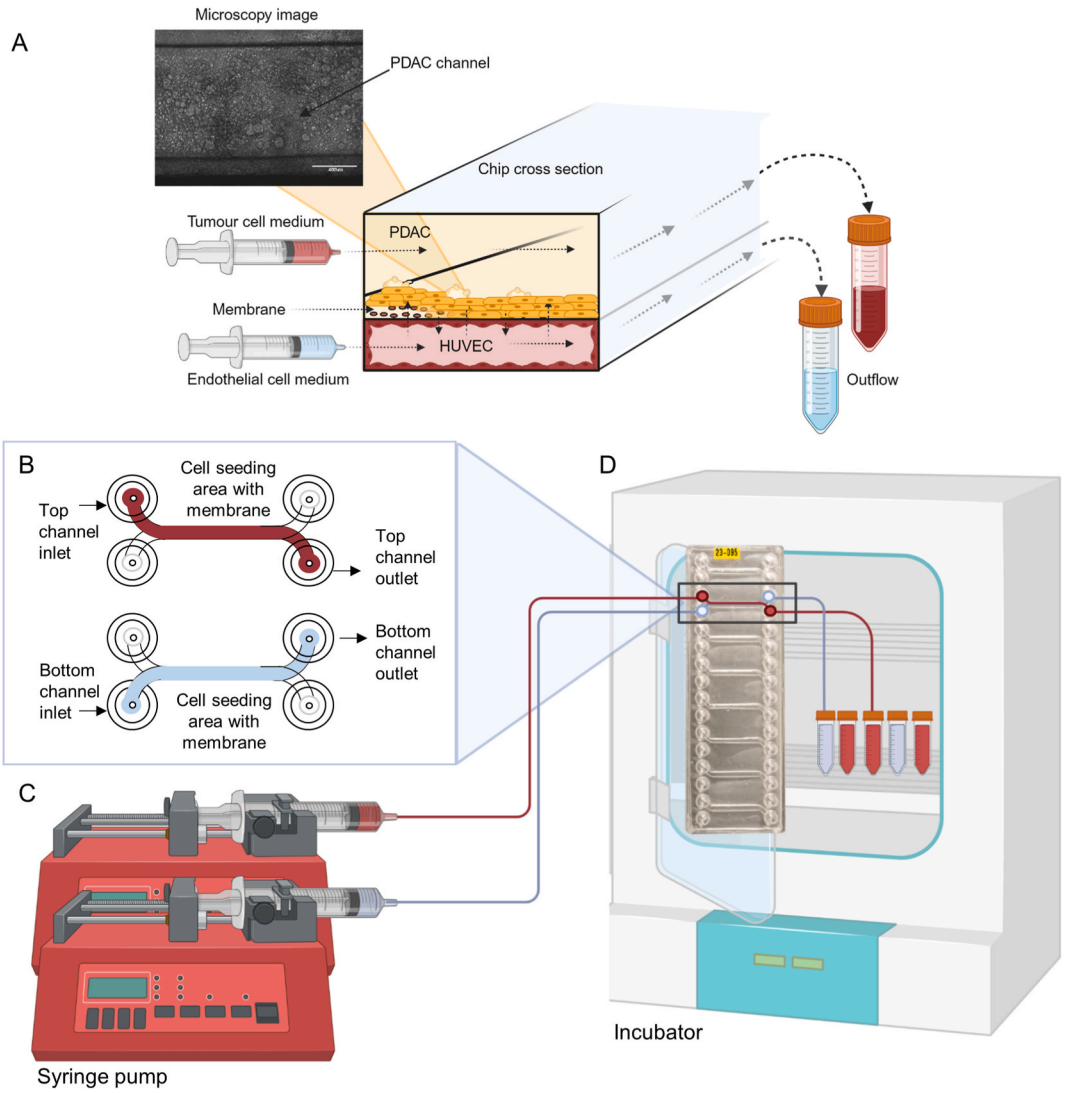

Fig. 1. PDAC chip setup scheme. (A) An illustration of the chip cross section with primary pancreatic ductal adenocarcinoma (PDAC) tumour cells in the upper channel and endothelial (HUVEC) cells in the bottom channel separated by a porous PET membrane. A brightfield image of the PDAC chip channel. (B) A diagram showing the flow direction in upper and bottom channels of the chip with the cell seeding membrane area highlighted. (C, D) A schematic of the microfluidic setup with the chip and outflow collection tubes in the incubator.

2.6. Immunolabelling of tumor hPOs and cells on the chip

Immunofluorescence analysis was performed on tumour hPO cryosections, whole mount-prepared tumour hPOs and chip membranes. Tumour hPO cultures were washed with PBS and fixed in 4% paraformaldehyde (PFA) with 100 mM sucrose for 30 min. For cryosectioning, organoids were subsequently incubated in 30% sucrose PBS solution overnight at 4°C, pelleted and frozen in optimal cutting temperature solution (Sakura Finetek). 10 μm-thick frozen sections were used for immunolabelling. For whole-mount imaging, organoids were prepared according to the previously published protocol [42]. For chip membrane immunofluorescence, cells in the chip were fixed with 4% PFA using 4 μl/min perfusion and washed with PBS. Membranes were extracted, cut into several fragments, and used for immunolabelling in a 24-well plate. Labelled membrane fragments were mounted on a glass slide in a mounting medium and subjected to microscopy.

The following antibodies were used: epithelial marker E-cadherin (CDH1) (BD Biosciences, #610182), endothelial marker VE-cadherin (CD144), ductal marker Cytokeratin 19 (CK19) (Dako/Agilent, #M0888), pancreatic progenitor markers SOX9 (EMD Millipore #Ab5535), PDX1 (R&D Systems, #AF2419), pancreatic tumour markers GATA6 (Cell Signaling Technology, #5851S) and Mucin 5AC (MUC5AC), (Santa Cruz Biotechnology, Inc. SC21701), apoptosis marker Cleaved Caspase-3 (Cell Signaling Technology, #9661), Anti-mouse IgG Donkey Alexa Fluor™ Plus 488 (Thermofisher, #A32766) Anti-rabbit IgG Donkey Alexa Fluor™ Plus 555 (Thermofisher, #A32794), Anti-goat IgG CF™ 647 (Sigma Aldrich #SAB4600175). Bright-field images were acquired using an EVOS digital light microscope (Thermo Fisher Scientific). Immunofluorescence images were obtained using a fluorescent live-imaging microscope (Till Photonics) Images were subsequently analysed using ImageJ software (National Institutes of Health) and QuPath [43].

2.7. Cell barrier permeability tests in the chip

Cascade Blue (#C687, Invitrogen TM) was prepared in EndoGRO-VEGF Complete Culture (#SCME002, Millipore) media with a concentration of 50 μg/ml. The media flow was stopped and new syringes with cascade blue in EndoGRO VEGF media with a total of 4 ml were added to the pump, set to different flow rates – 1 μl/min, 2 μl/min and 4 μl/min and placed in the incubator. After the incubation time, the outflow media was collected from both channels and 100 μl volume per sample

was transferred to a 96-well plate. The fluorescence was read at 400/420 nm using a Tecan Infinite 200 spectrophotometer and results were analysed using Graph Pad Prism software (Dotmatics). For the calculation of the apparent permeability, we adopted the barrier function analysis by Emulate [44] (Emulate). The following formula was used to calculate the apparent permeability:

$$P_{app} = -\frac{Q_T{*}Q_B}{SA{*}(Q_T{*}Q_B)}{*}ln\left[1-\frac{C_{T,0}{*}(Q_T+Q_B)}{(Q_T{*}C_{T,0}+Q_B{*}C_{B,0})}\right]$$

The P_{app} in the formula is the apparent permeability (cm/s), SA is the cell contact surface area separated by a membrane (cm^2), Q_T and Q_B are the flow rates in the top (tumour) and bottom (endothelial) channels (cm^3/s), while $C_{T,0}$ and $C_{B,0}$ are the concentrations measured in the outflows of the top and bottom channels respectively (μM).

2.8. Cell viability LDH detection assay in the chip outflows

The cytotoxicity was estimated by measurement of tissue damage marker lactate dehydrogenase (LDH) activity by a colourimetric assay (LDH-Cytotoxicity Assay Kit II, Sigma-Aldrich, cat.nr.MAK380). The aspirated or outflow cell culture media were collected, centrifuged at 600×*g* for 10 min and transferred in a 96-well microplate at 10 μl/well. 100 μl of LDH reaction mix was added to cell culture media per well and LDH activity was measured according to the manufacturer's instruction. The absorbance measurement was performed at a wavelength of 450 nm using a microplate reader (Tecan Infinite M200Pro, Tecan Trading AG, Männedorf, Switzerland).

2.9. Chip outflow secretome analysis using multianalyte detection assay (multiplex)

PDAC chip outflow samples were analysed for a variety of cytokines using the Human ProcartaPlex™ Mix&Match panel (Invitrogen, USA) according to the manufacturer's instructions. The following analytes were detected: sAXL, CA19-9, Fractalkine (CX3CL1), MIC-1 (GDF-15), ICAM-1, Osteopontin, TIMP-1. Fractalkine was detected as a soluble secreted apoptotic marker [45]. In turn, the carbohydrate antigen 19.9 (CA-19.9) is the best-established biomarker used in PDAC clinical management. CA-19.9 exhibits a strong correlation with pancreatic disease and elevated levels are indicative of worse overall survival [46]. Many other promising candidates are emerging, for example, osteopontin and TIMP-1, that can distinguish PDAC from pancreatitis [47]. Some biomarkers, like ICAM-1 and Macrophage inhibitory cytokine 1 (MIC-1, also known as GDF15), show a high level of specificity in combination with CA-19.9 [48,49] and can be used for early stage PDAC detection [49]. Other novel biomarkers, for instance, soluble AXL (sAXL), can outperform CA-19.9 in discriminating cancer from chronic pancreatitis [50]. Briefly, magnetic beads coupled with antibodies for 7 different analytes were added and washed twice with wash buffer. The standard was prepared by mixing solutions provided by the manufacturer, and a serial dilution protocol was used to prepare a range of standard solutions (1:3 serial dilution). Both standards and samples were prepared and added to the washed beads in the designated wells of the plate and incubated in an orbital shaker at 600 rpm for 2 h. Between incubations with different antibodies, the plate was washed twice with the wash buffer. The plate was then incubated with secondary antibodies for 30 min and with streptavidin-RPE-coupled detection antibodies for 30 min. The plate was washed three times, resuspended in a reading buffer, and analysed using a MAGPIX® instrument (Luminex Corporation, USA).

2.10. Imaging flow cytometry

Flow cytometry data were acquired using Amnis® ImageStream®XMark II (Luminex). The acquisition was performed using 488 and 642 lasers set to 100 mW and 5 mW power respectively. EpCAM-FITC (BD Biosciences # 347197), CD90-FITC (BD Biosciences #555595) antibody and DRAQ5 DNA probe were used. Gating was performed based on event size and signal in Ch5 (DRAQ5) using unstained samples as controls. Data were acquired using the INSPIRE® software and analysed using the IDEAS® software (Luminex).

2.11. Data analysis and presentation

Statistical analysis and data visualization were performed using GraphPad Prism software (GraphPad Prism Software V8.0, USA). Student's t-test with Welch's correction was used and P-values less than 0.05 were considered significant. All the data in bar graphs are presented as mean ± SD, while in whisker plots, whiskers denote min. and max. values. Figs. 1–3 were partially created with BioRender.com.

3. Results

1 Microfluidic pancreatic tumour chip setup

The microfluidic device we produce to create a personalized pancreatic ductal adenocarcinoma (PDAC) chip has a vertically stacked design. It consists of eight pairs of channels separated by a 20 μm thick porous PET membrane that would represent the proximity of PDAC to the vasculature in tumour conditions (Fig. 1A). Inlets were used for cell seeding and perfusion – the top channel was used for tumour cells and the bottom channel for endothelial cells (Fig. 1A and B). For high consistency and accuracy of the outflow reading, the fabrication protocol has specifically been tailored for the fabrication of PDMS-free microfluidic chips, thus ensuring that the lipophilic molecule absorption of PDMS is avoided.

PDMS despite being a heavily used material in microfluidics research has critical drawbacks from the small molecule absorption perspective [51,52]. Furthermore, the lack of highly repeatable and mass manufacturing-compatible device fabrication process, has resulted in Organ on Chip standardization group [53] setting forward a goal to move towards PDMS-free chip technology. Herein used OSTE and COC combines easy to fabricate devices [54] with COC polymer that counters the optical scattering observed in OSTE-only devices [55]. One of the core tenets for the chip design was continuous perfusion of the media for both epithelial and endothelial designs, which has been heavily used in studying other cancer models [56]. Furthermore, the design allows for independent media sampling as well as non-invasive barrier integrity evaluation [44].

The microfluidic setup consisted of a syringe pump with a flow controller located outside of the incubator (Fig. 1C and D). To avoid shear stress fluctuations, typically seen in peristaltic systems, syringe pumps were used throughout the study, which, however, required frequent syringe exchanges due to linear velocity restrictions seen with the use of 10 ml and 20 ml syringes, which typically have internal diameters exceeding 15 mm.

2 Characterisation of primary tumour organoids to be used for the PDAC chip

Next, using the organoid culture approach, we expanded and characterized the primary tumour resection material to be used in the PDAC chips. PDAC is a desmoplastic tumour that can have a relatively low tumour cell concentration and a significant stromal component [8]. Recently, protocols have emerged for generating primary human pancreatic organoids (hPOs), enabling the establishment of both normal pancreatic duct organoids and tumour hPOs [18,19]. The culture of digested primary PDAC tissue proved a good tool to enrich pure neoplastic cell populations without stromal components [19].

We first generated hPOs from PDAC tumour tissue (Fig. 2A) and characterized them using immunofluorescence and targeted DNA

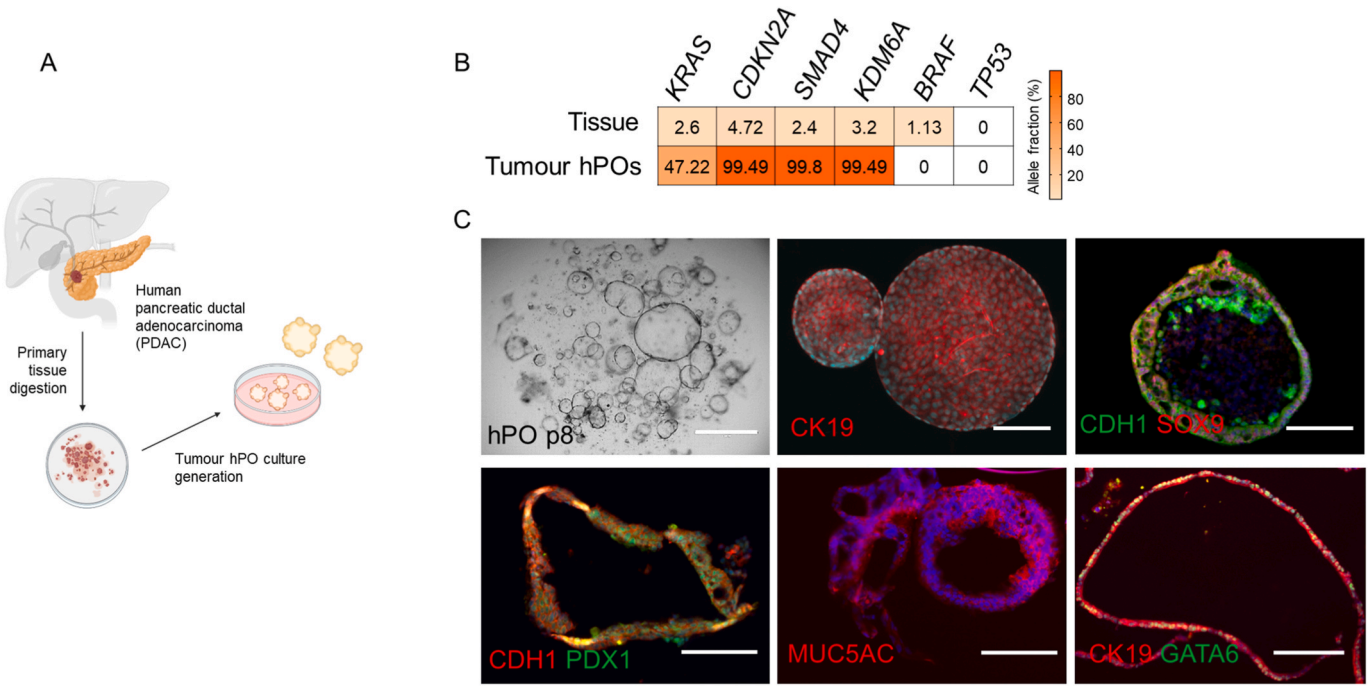

Fig. 2. Generation and characterisation of human pancreatic tumour organoids (hPOs). (A) Tumour hPOs were isolated from the donor material obtained during a tumour resection procedure. (B) An allele fraction heat map showing pathogenic mutations identified by targeted DNA sequencing in the original donor tissue and tumour hPOs expanded to passage five. (C) Microscopy images of the corresponding tumour hPOs. A bright-field image of a gel dome containing tumour hPOs and immunofluorescent images of a whole-mount (CK19) and cryo section preparations showing the expression of epithelial (CDH1, CK19), pancreatic progenitor (PDX1, SOX9) and tumour (MUC5AC, GATA6) markers. Scale bars – 100 μm.

sequencing to prove their tumour identity, since there is no single reliable marker for all PDAC subtypes. We selected a tumour hPO line that harboured several hallmark PDAC pathogenic mutations, notably in the *KRAS*, *CDKNA2* and *SMAD4* genes (Fig. 2B). When compared to the mutation profile of the original tissue, we found that the mutation in *BRAF* was detected in the tissue sample but not in the cultured tumour hPOs. This could be due to culture selection against certain clones, which is in line with previous findings [19,20]. Of note, the allele fraction of the identified pathogenic mutations increased with culture further suggesting the enrichment of tumour cells with the set mutation status (Fig. 2B). Other genes frequently affected in PDAC (e.g. *TP53, ARID1A, BRCA2, GNAS, MYC*) were included in the sequencing, but were found not to be aberrant in the assay we performed.

Immunofluorescent analysis of the selected tumour hPO line (Fig. 3C) revealed widespread expression of the epithelial marker E-cadherin (CDH1), the ductal marker Cytokeratin 19 (CK19), as well as pancreatic progenitor markers PDX1 and SOX9. Apart from the pancreatic ductal phenotype markers, the cells were positive for pancreatic tumour markers MUC5AC and GATA6, suggesting the Classical PDAC subtype. Additionally, purity analysis of the hPO line to exclude fibroblast contamination was performed (Fig. S1). Taken together, these data suggest the PDAC nature of the hPO line selected for further experiments and outlines a general workflow for the characterisation of the material for the personalized chip, that should include phenotypic analysis and a sequencing approach.

3 Functionality of the PDAC chip with an endothelial cell barrier

To create a PDAC chip with an endothelial cell barrier, we first populated the device with human umbilical vein endothelial cells (HUVECs). Normally, by day four on the chip, HUVECs reached full confluence and dissociated tumour hPOs were subsequently seeded in the upper channel of the device. The culturing of both channels was continued, before collecting the cells for immunolabelling, as shown in the experimental timeline (Fig. 3A). A PDAC chip with outflows running separately could be maintained in culture for more than 50 days. We chose to dissociate the tumour hPOs to recapitulate the nature of the pancreatic duct lumen, which is also best compatible with the chip design we use and would allow channel-specific outflow collection. Previously, Haque and colleagues have described a microfluidic chip that sustained the survival of primary pancreatic organoids in the gel compartment for more than 26 days. The chip consisted of an organoid compartment and a channel providing a culture medium with constant flow. Interestingly, within a week, organoids seeded on the chip in Matrigel nevertheless lost their spherical structure and grew as adherent cell layers [36].

To confirm that dissociated organoids maintain a PDAC identity, we characterised them on the chip. The cells grew adherently, forming monolayer first, with a morphology resembling that of adherent cultures in the tissue culture dishes (Fig. 3B). When cultured for a longer period, the tumour cell layer became denser and displayed some vertical growth, as apparent from the brightfield images (Fig. 3C). Dissociated organoids on the chip retained the expression of the pancreatic ductal (CK19, CDH1), progenitor (PDX1, SOX9) observed in the tumour hPO cultures and expressed tumour markers (GATA6), as assessed by immunofluorescence (Fig. 3D). The cells on the chip remained CK19-positive beyond day 50 (Fig. 3E.). Moreover, we observed detachment of overgrowing cells that could be detected in the outflow (Fig. 3F).

Other studies employed primary tumour hPOs to successfully study PDAC interaction with the tumour microenvironment in two- [34] and three-channel [35] multi-chip plates. In those studies, the tumour organoids grew in a gel compartment and the flow was ensured by placing the plate on the rocker and driven by plate inclination. The use of basement-membrane matrices such as Matrigel is common since it provides mechanical cues and rich conditions for organoid cultures. Nevertheless, it is associated with potential limitations due to variations in gel content and properties that can have effects on organoid phenotype and cell sensitivity to chemical compounds [57,58]. An earlier report studied the hypovascularity of pancreatic ductal adenocarcinoma (PDAC) using a biomimetic chip to demonstrate how tumour cells ablate

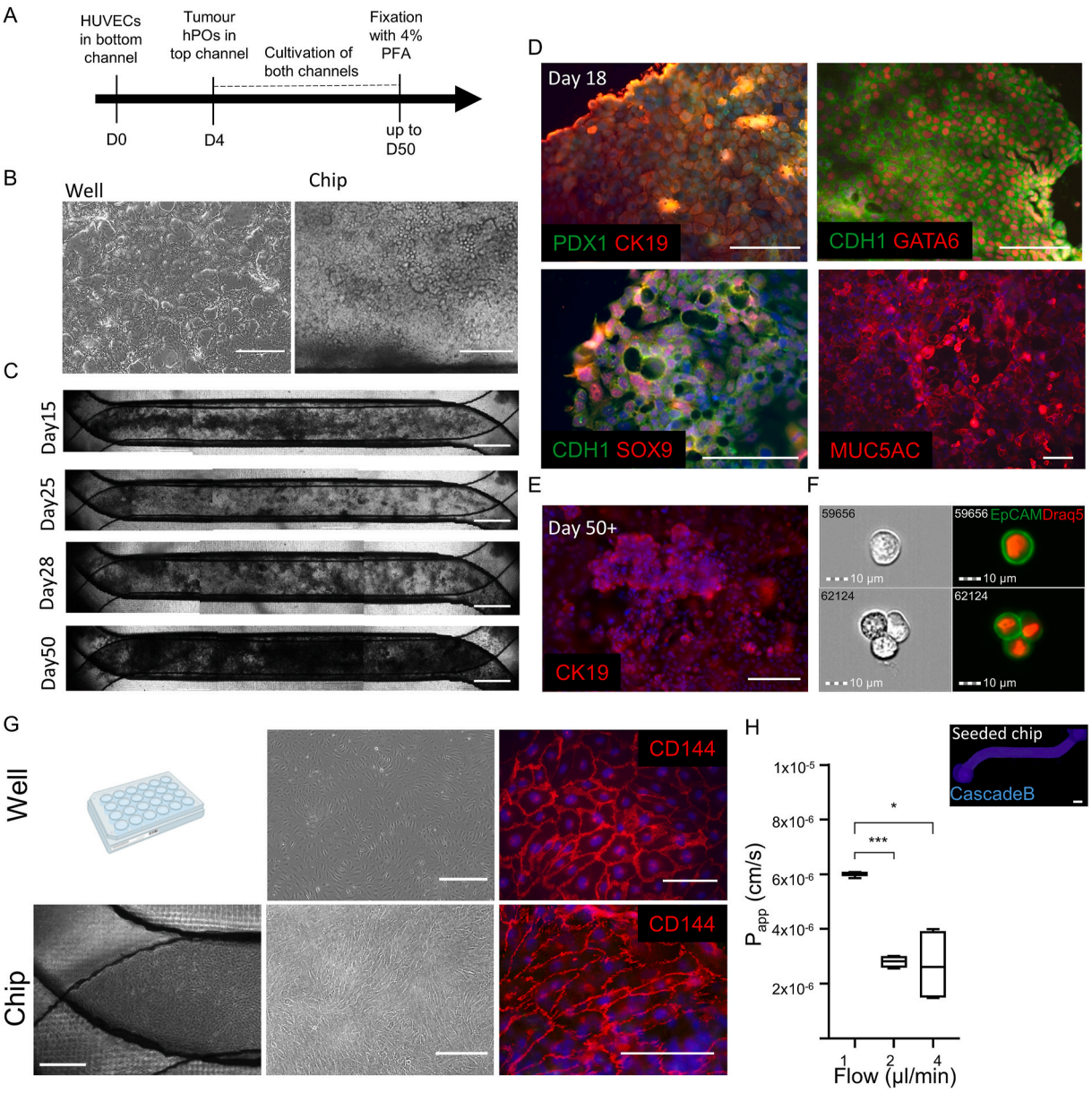

Fig. 3. Functional characterisation of the PDAC chip. (A) A diagram depicting cell seeding and cultivation timeline for the PDAC chip. (B) Bright-field images of the dissociated hPOs seeded in the tissue culture plate well and on the chip membrane. (C) A series of bright-field images of the hPOs on the PDAC chip taken from the same channel at different time points. (D) Immunofluorescent phenotyping of the dissociated tumour hPOs on the chip membrane fixed at D18. (E) Tumour hPO cells on the chip after more than 50 days of culture labelled with anti-CK19 antibody. (F) EpCAM-positive cells detected in the tumour channel outflow of the PDAC chip. (G) HUVEC cell morphology and immunophenotyping on the plate and in the chip. (H) Apparent permeability (P_{app}) values for the endothelial/epithelial barrier of the PDAC chip under various flow rate conditions obtained using cascade blue (n = 3 channels). A fluorescent image of the cascade blue visible in the bottom channel of a PDAC chip under 4 µl/min flow rate. Scale bars: (B) – 400 µm; (D,E) – 100 µm; (G) – 400 µm for bright-field images, 100 µm for fluorescent; (H) – 1000 µm. *P < 0.05, ***p < 0.001 (n = 3-6).

blood vessel cells [38]. The PDMS-based chip contained a collagen-filled chamber with two hollow channels, which were populated with murine pancreatic cancer cells (PD7591) and HUVECs. Here as well, the endothelial perfusion was achieved via gravity-driven media flow. Unlike in the mentioned studies, we used a PDMS-free chip coupled with a syringe pump to the advantage of having controlled constant flow to mimic blood vessel and ductal perfusion.

HUVECs on the chip and in the culture dish exhibited similar morphology and expressed characteristic markers, such as VE-cadherin (Fig. 3G). An essential feature of microfluidic devices with an endothelial barrier is the possibility to assess the permeability of this barrier, which allows to evaluate its capacity to mimic in vivo conditions [59]. To determine the permeability of the endothelial layer, we applied cascade blue (CB) in the bottom channel at various flow rates and attempted to detect the fluorescent compound in the outflow of the upper PDAC channel. We detected a marked increase in the concentration of CB in the epithelial channel at lower flow rates. The apparent permeability (P_{app}) under a 1 µl/min flow rate increased more than two-fold compared to the 2 and 4 µl/min flow conditions (Fig. 3H).

The permeability of the endothelial barrier depends on several biological and physical parameters, including the composition of the intercellular junctions and the shear stress experienced by the cells [60,61]. Shear stress can affect blood vessel development, maturation and permeability. These effects, however, are context-dependent and can be influenced by many factors, including the extracellular matrix composition as well as the nature (stable vs. oscillating) and duration of shear

stress [61–63]. In vivo, higher levels of stable shear stress correlate with decreased blood vessel permeability [61]. Our observations in the chip are in line with this narrative and suggest reduced permeability in higher flow rate settings, which are characterised by increased shear stress [64,65].

Taken together, we demonstrate that primary PDAC tissue initially expanded as tumour hPOs, can be subsequently cultured for a prolonged period as adherent cells in the OOC device in close contact with endothelial cells. Continuous monitoring of cell morphology and collection of separate outflows from tumour and endothelial channels are possible in these settings. Additionally, the system provides the opportunity to modulate the flow and permeability parameters of the endothelial barrier. The chip could be further developed by incorporating additional stromal components, such as fibroblasts and glial cells, to better mimic the PDAC microenvironment or to model processes like metastasis formation and perineural infiltration.

4 Viability of the HUVEC and PDAC cells on the chip

To further characterise the cells on the chip, we analysed tumour hPO and HUVEC cell viability using several approaches. The advantage of the chip design we employ is the ample amount of the outflow medium readily available for analysis. We used lactate dehydrogenase (LDH) as a readout for the well-being of the cells on the PDAC chip and compared it to standard adherent cell culture conditions. In both settings for confluent cell layers, we noted higher levels of LDH in tumour hPO cells compared to HUVEC cells with greater LDH level fluctuation in the case of tumour samples (Fig. 4A and B). Of note, we also detected fluctuations in the density of the hPO cells on the chip over the same period (Fig. S2). Additionally, to explore the option of using secreted apoptotic signal detection in OOC outflows, we selected CX3CL1 (fractalkine), an early apoptosis chemokine that has been reported to act as a "find-me" signal [45]. In line with the LDH data, fractalkine could be detected at higher concentrations in tumour cell conditioned medium and channel outflows than in HUVEC samples (Fig. 4C and D). Moreover, like for LDH, the levels of fractalkine combined from tumour and endothelial channels, increased with cultivation time on the chip (Fig. 4E). These observations were further supported by immunofluorescent detection of Caspase3 in tumour and HUVEC cells, where noticeable levels of the apoptosis marker were found in PDAC samples (Fig. 4F and G). A simple outflow-based readout would be more convenient if continuous viability monitoring in the chip is desired. LDH can be used to measure cell viability but is a sign of necrosis. Here, in addition to cell death detection, we propose to monitor the secretion of "find-me" or "eat-me" signals as early signs of apoptosis, which, to our knowledge, has not been adopted for chip applications.

An important limitation of the presented data, and a broader challenge in the field, is the difficulty of normalising the detected analytes in a running chip, especially in dense cultures with 3D structures. Ideally, this would require a soluble molecule secreted by tumour or other specific cell type (e.g. in case of co-culture with stromal cells), which would correlate with cell density and could be reliably detected in the

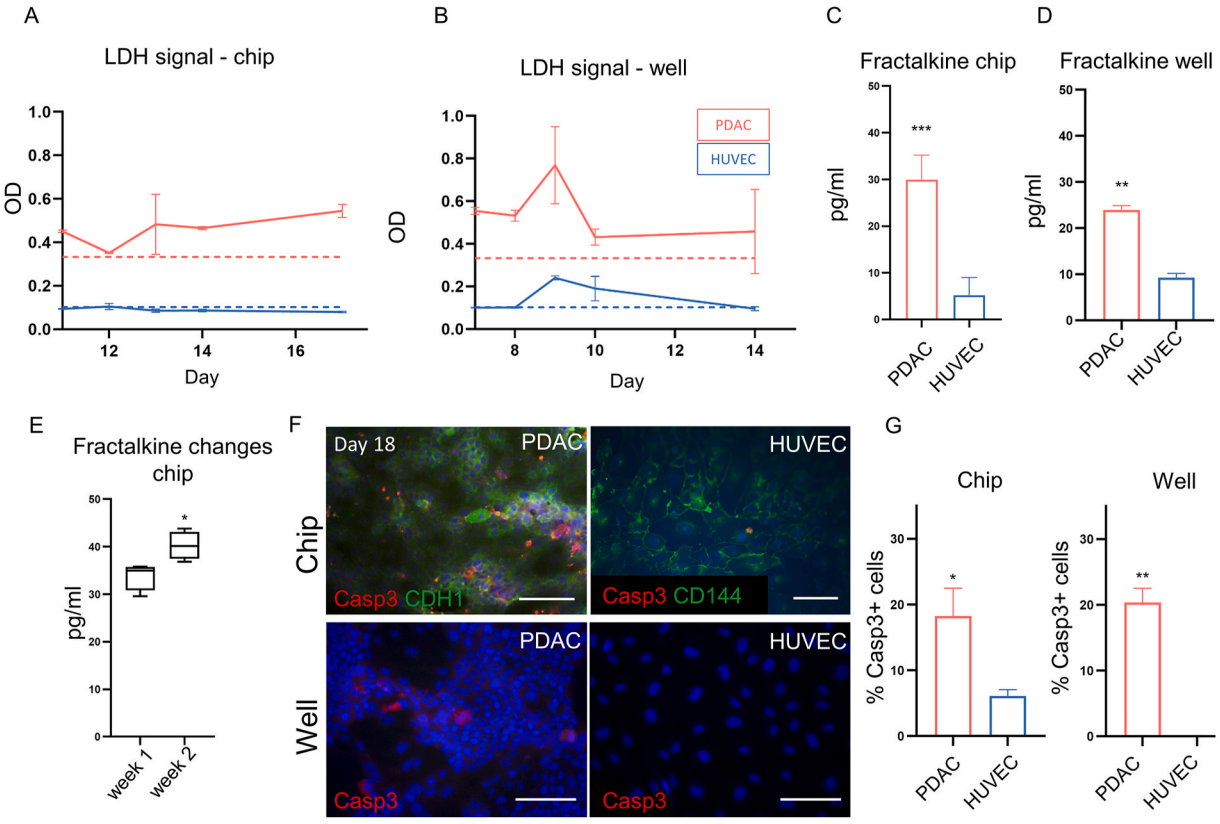

Fig. 4. Cell viability on the PDAC chip. LDH signal detected in the chip outflows (A) and conditioned media from the tissue culture wells (B) in tumour hPO (red line) and HUVEC (blue line) samples, displayed as optical density (OD) values (the dotted line represents LDH signal derived from the respective fresh media). Fractalkine concentration values detected in the PDAC chip outflows (C) and conditioned media from the tissue culture wells (D). (E) Combined values of the fractalkine concentration levels detected in both pancreatic tumour and HUVEC channel outflows of the PDAC chip, measured at different time points one week apart. (F) Representative immunofluorescence images of Caspase 3 staining performed on pancreatic tumour and HUVEC cells on the chip and in the tissue culture wells. (G) Quantification of the Caspase 3 staining in dissociated tumour hPOs and HUVEC in the well and on the chip. Number of replicates (n): (A) n = 4 replicates from two individual channels for each condition. (B) n = 2 wells for each condition; (C) n = 9 measurements at different time points from a total of 5 channels across 2 chips for each condition; (E) n = 4 channels from 2 chips; (G, left panel) high magnification images from 3 individual PDAC and HUVEC channels. (G, right panel) n = 3 high magnification images from 3 different PDAC/HUVEC wells; Scale bars – 100 μm. *P < 0.05, **P < 0.01, ***p < 0.001.

outflow. Additionally, a standard curve to correlate cell numbers would need to be established for each cell type. Alternatively, a non-invasive method, such as transepithelial electrical resistance (TEER) measurements, could be integrated into the system to quantify cell density.

5 Comparison of the secretory pancreatic cancer biomarkers in the PDAC chip and conventional 2D cell culture

A common justification for the benefit of microfluidic chips is their enhanced ability to recapitulate the organ microenvironment and overall in vivo conditions. Given the successful detection of the apoptotic biomarker fractalkine, we further focused on the outflow analysis to detect other potentially relevant PDAC biomarkers.

We designed a panel that includes these markers and performed a multianalyte detection assay on the PDAC chip outflows of both endothelial and tumour hPO channels at different time points (Fig. 5A and B). Conditioned medium from tissue culture dishes was used as a reference (Fig. 5C). Our analysis demonstrated that all the tested biomarkers could be detected in the chip outflows (Fig. 5A and B; Supplementary Table 1). As expected, we observed significantly higher levels of ICAM-1 and Osteopontin in both PDAC-conditioned media and chip outflows compared to endothelial samples. Likewise, in the microfluidic settings,

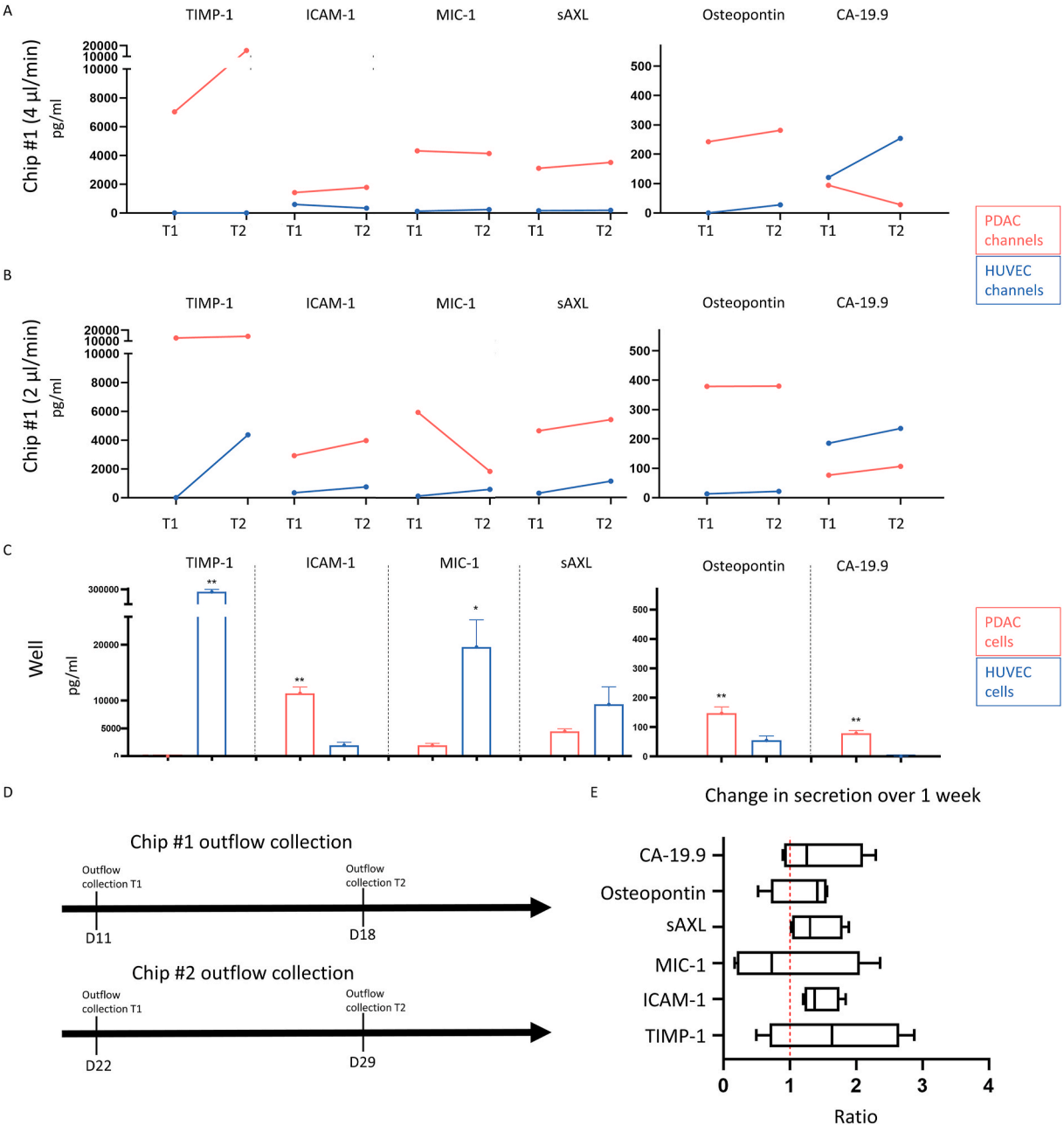

Fig. 5. PDAC biomarker analysis. Concentration means of various PDAC biomarkers detected at different time points (T1 and T2) in tumour hPO (blue lines) and HUVEC (red lines) channel outflows in two different chip setups. (A) Chip #1 was cultured at a 2 µl/min flow rate and outflows collected at T1 = D11, and T2 = D18. (B) Chip #2 was cultured at a 4 µl/min flow rate, outflows collected at T1 = D22, and T2 = D29. (C) Biomarker concentration in the conditioned medium from the tumour hPOs (red bars) and HUVECs (blue bars) cultivated as adherent cells in tissue culture wells. (D) A diagram showing the outflow collection time points (T1 and T2) for each chip. (E) The changes in biomarker concentration in both tumour and HUVEC outflows combined, expressed as the ratio between concentration detected on T2 vs. T1. Number of replicates (n): (A) n = 1 channel outflow at T1 and n = 2 channel outflows at T2 for each condition; (B) n = 3 channel outflows at T1 and T2 for each condition; (C) conditioned media from n = 3 wells analysed for each condition. (E) n = 4 channels across two chips. *P < 0.05,**P < 0.01, ***P < 0.001.

the majority of TIMP-1 could specifically be detected in tumour channel outflows. Strikingly, however, virtually no TIMP-1 was detected in the culture medium collected from tumour hPO cells on the dish, whereas conventionally cultured HUVECs displayed high secretion, with up to 300 ng/ml detected in the medium. A similar reverse pattern was observed for MIC-1 and soluble AXL (sAXL). These proteins were abundant in HUVEC-conditioned medium, while in microfluidic settings, they were predominantly detected in the PDAC channel outflows.

CA-19.9 was detected almost exclusively in the PDAC-conditioned medium. On the chip, however, the majority of this glycoprotein was detected in the endothelial channel outflows. This could represent an intrinsic change in HUVECs that are challenged by different culture conditions. Alternatively, some of the secreted products from PDAC cells could cross the endothelial barrier, representing the endothelial channel-directed secretion of the analyte.

To corroborate the finding, we repeated the biomarker detection in a separate chip with different flow rates and observed robust similar secretion patterns within a comparable range (Fig. 5B). The time points used for the outflow collection on both chips are depicted in the diagram in Fig. 5D. Additionally, we assessed the changes in biomarker secretion over one week of culture on the chip and found that, collectively, the secretion of the tested biomarkers tends to increase over time. For some analytes, like sAXL and ICAM-1, there was a significant increase in secretion (Fig. 5E).

Previously, the detection of various biomarkers has been demonstrated in microfluidic OOC outflows using conventional detection methods and integrated technologies or sensors [66,67]. A common problem for the detection of biomarkers on the chip is their low abundance often below the detection threshold [67]. Our observations validate that chip outflows can be successfully used for the detection of PDAC biomarkers. Moreover, we identified significant discrepancies between the conventional adherent culture conditioned media and chip outflows – four out of six analytes displayed reverse secretion patterns in the tested conditions, which supports our hypothesis that the PDAC chip represents the physiological conditions of the tumour microenvironment more closely.

Overall, the search for novel biomarkers holds promise for the early PDAC detection and conception of population screening programs [7]. However, biomarkers could also help guide therapy decisions and their detection in microfluidic tumour models could be an asset for personalized medicine approaches [68]. Intriguingly, in a recent prospective study, involving experimental validation in cell lines and primary organoids, NDUFB8 and CEMIP2 were found to be predictive of an adjuvant therapy response in PDAC patients [69].

4. Conclusions

Here we describe a workflow for establishing a personalized PDAC chip using tumour hPOs and HUVECs as endothelial counterpart, that recapitulates the physiological vascular barrier and tumour interaction in a OOC system. The novelty of our platform is the use of a PDMS-free chip coupled with a syringe pump that offers the advantage of controlled constant flow to mimic blood vessel perfusion. Moreover, we also provided the flow in the pancreatic channel. In our setup, the PDAC tissue expanded as hPOs can be further cultured as adherent cells on the chip for more than 50 days with continuous monitoring of cell viability using tumour and endothelial channel outflows. The data suggest a gradual increase in cell density and turnover of cells in the tumour channel. We demonstrate that several tumour-specific biomarkers such as CA-19.9, TIMP-1, Osteopontin, MIC-1, ICAM-1 and sAXL could be reliably detected in the collected chip outflows. Additionally, we compare biomarker secretion patterns in tissue culture plates and microfluidic conditions and detect major discrepancies suggesting the benefit of the chip approach.

The described personalized PDAC chip could be used for improved drug sensitivity assays and serve as a platform for studying biomarker secretion for precision medicine applications. We envision that the PDAC chip could be further developed by adding tumour microenvironment counterparts to subsequently study various aspects of tumour biology. It would be suitable for studies on metastasis initiation, drug-induced vascular damage, as well as the impact of vasculature deprivation and hypoxia on drug delivery.

Furthermore, the two compartment chip design could be used to study other biologically relevant barrier functionality in OOC models of blood-brain barrier, placenta, lung, gut, kidney, skin and oral mucosa. Up to 8 vertically stacked models could be placed on the chip and interconnected through small tubing and standardized mini-luer connectors serving as a platform for multi-organ chip models.

Funding sources

The study was financially supported by the Latvian Council of Science State Research Programme project “Smart Materials, Photonics, Technologies and Engineering Ecosystems” (VPP-EM-FOTONIKA-2022/1-0001). The Institute of Solid-State Physics, University of Latvia as the Center of Excellence has received funding from the European Union’s Horizon 2020 Framework Programme H2020-WIDESPREAD-01-2016-2017-TeamingPhase2 under grant agreement No. 739508, project CAMART2.

CRediT authorship contribution statement

Karina Goluba: Writing – original draft, Visualization, Methodology, Investigation, Formal analysis, Data curation. **Vadims Parfejevs:** Writing – review & editing, Writing – original draft, Visualization, Methodology, Investigation, Funding acquisition, Formal analysis, Data curation, Conceptualization. **Evita Rostoka:** Validation, Methodology, Formal analysis, Conceptualization. **Kaspars Jekabsons:** Software, Investigation, Formal analysis. **Ilze Blake:** Investigation, Formal analysis. **Anastasija Neimane:** Investigation, Formal analysis. **Annija Anete Ule:** Resources, Methodology. **Roberts Rimsa:** Writing – review & editing, Writing – original draft, Visualization, Resources, Methodology, Funding acquisition, Conceptualization. **Reinis Vangravs:** Resources, Investigation. **Andrejs Pcolkins:** Resources. **Una Riekstina:** Writing – review & editing, Writing – original draft, Supervision, Project administration, Funding acquisition, Conceptualization.

Declaration of competing interest

The authors declare that they have no known competing financial interests or personal relationships that could have appeared to influence the work reported in this paper.

Data availability

Data will be made available on request.

Appendix A. Supplementary data

Supplementary data to this article can be found online at https://doi.org/10.1016/j.mtbio.2024.101262.

References

[1] J. Kleeff, M. Korc, M. Apte, C. La Vecchia, C.D. Johnson, A.V. Biankin, et al., Pancreatic cancer, Nat Rev Dis Primers 2 (2016) 16022, https://doi.org/10.1038/nrdp.2016.22.
[2] Y. Jiang, D.P.S. Sohal, Pancreatic adenocarcinoma management, JCO Oncol Pract 19 (2023) 19–32, https://doi.org/10.1200/OP.22.00328.
[3] A.E. Becker, Y.G. Hernandez, H. Frucht, A.L. Lucas, Pancreatic ductal adenocarcinoma: risk factors, screening, and early detection, World J. Gastroenterol. 20 (2014) 11182–11198, https://doi.org/10.3748/wjg.v20.i32.11182.

[4] S. Rahn, V. Zimmermann, F. Viol, H. Knaack, K. Stemmer, L. Peters, et al., Diabetes as risk factor for pancreatic cancer: hyperglycemia promotes epithelial-mesenchymal-transition and stem cell properties in pancreatic ductal epithelial cells, Cancer Lett. 415 (2018) 129–150, https://doi.org/10.1016/j.canlet.2017.12.004.

[5] L. Rahib, B.D. Smith, R. Aizenberg, A.B. Rosenzweig, J.M. Fleshman, L. M. Matrisian, Projecting cancer incidence and deaths to 2030: the unexpected burden of thyroid, liver, and pancreas cancers in the United States, Cancer Res. (2014), https://doi.org/10.1158/0008-5472.CAN-14-0155.

[6] A.S. Quante, C. Ming, M. Rottmann, J. Engel, S. Boeck, V. Heinemann, et al., Projections of cancer incidence and cancer-related deaths in Germany by 2020 and 2030, Cancer Med. 5 (2016) 2649–2656, https://doi.org/10.1002/cam4.767.

[7] S.P. Pereira, L. Oldfield, A. Ney, P.A. Hart, M.G. Keane, S.J. Pandol, et al., Early detection of pancreatic cancer, The Lancet Gastroenterology & Hepatology 5 (2020) 698–710, https://doi.org/10.1016/S2468-1253(19)30416-9.

[8] C.J. Halbrook, C.A. Lyssiotis, M. Pasca di Magliano, A. Maitra, Pancreatic cancer: advances and challenges, Cell 186 (2023) 1729–1754, https://doi.org/10.1016/j.cell.2023.02.014.

[9] R.A. Moffitt, R. Marayati, E.L. Flate, K.E. Volmar, S.G.H. Loeza, K.A. Hoadley, et al., Virtual microdissection identifies distinct tumor- and stroma-specific subtypes of pancreatic ductal adenocarcinoma, Nat. Genet. 47 (2015) 1168–1178, https://doi.org/10.1038/ng.3398.

[10] V. Ruta, C. Naro, M. Pieraccioli, A. Leccese, L. Archibugi, E. Cesari, et al., An alternative splicing signature defines the basal-like phenotype and predicts worse clinical outcome in pancreatic cancer, Cell Reports Medicine 5 (2024) 101411, https://doi.org/10.1016/j.xcrm.2024.101411.

[11] P. Bailey, X. Zhou, J. An, T. Peccerella, K. Hu, C. Springfeld, et al., Refining the treatment of pancreatic cancer from big data to improved individual survival, Function (Oxf) 4 (2023) zqad011, https://doi.org/10.1093/function/zqad011.

[12] H.M. Kolbeinsson, S. Chandana, G.P. Wright, M. Chung, Pancreatic cancer: a review of current treatment and novel therapies, J. Invest. Surg. 36 (2023) 2129884, https://doi.org/10.1080/08941939.2022.2129884.

[13] S. Coppola, I. Carnevale, E.H.J. Danen, G.J. Peters, T. Schmidt, Y.G. Assaraf, et al., A mechanopharmacology approach to overcome chemoresistance in pancreatic cancer, Drug Resist. Updates 31 (2017) 43–51, https://doi.org/10.1016/j.drup.2017.07.001.

[14] P.P. Provenzano, C. Cuevas, A.E. Chang, V.K. Goel, D.D. Von Hoff, S.R. Hingorani, Enzymatic targeting of the stroma ablates physical barriers to treatment of pancreatic ductal adenocarcinoma, Cancer Cell 21 (2012) 418–429, https://doi.org/10.1016/j.ccr.2012.01.007.

[15] D. Thomas, P. Radhakrishnan, Tumor-stromal crosstalk in pancreatic cancer and tissue fibrosis, Mol. Cancer 18 (2019) 14, https://doi.org/10.1186/s12943-018-0927-5.

[16] A. Letai, P. Bhola, A.L. Welm, Functional precision oncology: testing tumors with drugs to identify vulnerabilities and novel combinations, Cancer Cell 40 (2022) 26–35, https://doi.org/10.1016/j.ccell.2021.12.004.

[17] J. Kim, B.-K. Koo, J.A. Knoblich, Human organoids: model systems for human biology and medicine, Nat. Rev. Mol. Cell Biol. 21 (2020) 571–584, https://doi.org/10.1038/s41580-020-0259-3.

[18] L. Broutier, A. Andersson-Rolf, C.J. Hindley, S.F. Boj, H. Clevers, B.K. Koo, et al., Culture and establishment of self-renewing human and mouse adult liver and pancreas 3D organoids and their genetic manipulation, Nat. Protoc. 11 (2016) 1724–1743, https://doi.org/10.1038/nprot.2016.097.

[19] E. Driehuis, A van Hoeck, K. Moore, S. Kolders, H.E. Francies, M.C. Gulersonmez, et al., Pancreatic cancer organoids recapitulate disease and allow personalized drug screening, Proc. Natl. Acad. Sci. USA 116 (2019) 26580–26590, https://doi.org/10.1073/PNAS.1911273116.

[20] T. Seino, S. Kawasaki, M. Shimokawa, H. Tamagawa, K. Toshimitsu, M. Fujii, et al., Human pancreatic tumor organoids reveal loss of stem cell niche factor dependence during disease progression, Cell Stem Cell 22 (2018) 454–467.e6, https://doi.org/10.1016/j.stem.2017.12.009.

[21] M.K. Melzer, Y. Resheq, F. Navaee, A. Kleger, The application of pancreatic cancer organoids for novel drug discovery, Expert Opin Drug Discov 18 (2023) 429–444, https://doi.org/10.1080/17460441.2023.2194627.

[22] A. Rengaraj, L. Bosc, P. Machillot, C. McGuckin, C. Milet, N. Forraz, et al., Engineering of a microscale niche for pancreatic tumor cells using bioactive film coatings combined with 3D-architectured scaffolds, ACS Appl. Mater. Interfaces 14 (2022) 13107–13121, https://doi.org/10.1021/acsami.2c01747.

[23] J. Kokkinos, G. Sharbeen, K.S. Haghighi, R.M.C. Ignacio, C. Kopecky, E. Gonzales-Aloy, et al., Ex vivo culture of intact human patient derived pancreatic tumour tissue, Sci. Rep. 11 (2021) 1944, https://doi.org/10.1038/s41598-021-81299-0.

[24] C. Ricci, C. Mota, S. Moscato, D. D'Alessandro, S. Ugel, S. Sartoris, et al., Interfacing polymeric scaffolds with primary pancreatic ductal adenocarcinoma cells to develop 3D cancer models, Biomatter 4 (2014) e955386, https://doi.org/10.4161/21592527.2014.955386.

[25] P. Gupta, P.A. Pérez-Mancera, H. Kocher, A. Nisbet, G. Schettino, E.G. Velliou, A novel scaffold-based hybrid multicellular model for pancreatic ductal adenocarcinoma—toward a better mimicry of the in vivo tumor microenvironment, Front. Bioeng. Biotechnol. 8 (2020) 290, https://doi.org/10.3389/fbioe.2020.00290.

[26] F. Chiellini, D. Puppi, A.M. Piras, A. Morelli, C. Bartoli, C. Migone, Modelling of pancreatic ductal adenocarcinoma in vitro with three-dimensional microstructured hydrogels, RSC Adv. 6 (2016) 54226–54235, https://doi.org/10.1039/C6RA08420F.

[27] M.V. Monteiro, M. Rocha, V.M. Gaspar, J.F. Mano, Programmable living units for emulating pancreatic tumor-stroma interplay, Adv Healthc Mater 11 (2022) e2102574, https://doi.org/10.1002/adhm.202102574.

[28] K. Müller, D.A. Fedosov, G. Gompper, Margination of micro- and nano-particles in blood flow and its effect on drug delivery, Sci. Rep. 4 (2014) 4871, https://doi.org/10.1038/srep04871.

[29] M.W. Dewhirst, T.W. Secomb, Transport of drugs from blood vessels to tumour tissue, Nat. Rev. Cancer 17 (2017) 738–750, https://doi.org/10.1038/nrc.2017.93.

[30] D.E. Ingber, Human organs-on-chips for disease modelling, drug development and personalized medicine, Nat. Rev. Genet. 23 (2022) 467–491, https://doi.org/10.1038/s41576-022-00466-9.

[31] K. Haase, R.D. Kamm, Advances in on-chip vascularization, Regen. Med. 12 (2017) 285–302, https://doi.org/10.2217/rme-2016-0152.

[32] V. Vickerman, J. Blundo, S. Chung, R. Kamm, Design, fabrication and implementation of a novel multi-parameter control microfluidic platform for three-dimensional cell culture and real-time imaging, Lab Chip 8 (2008) 1468–1477, https://doi.org/10.1039/b802395f.

[33] X. Liu, J. Fang, S. Huang, X. Wu, X. Xie, J. Wang, et al., Tumor-on-a-chip: from bioinspired design to biomedical application, Microsyst Nanoeng 7 (2021) 1–23, https://doi.org/10.1038/s41378-021-00277-8.

[34] M. Geyer, D. Schreyer, L.-M. Gaul, S. Pfeffer, C. Pilarsky, K. Queiroz, A microfluidic-based PDAC organoid system reveals the impact of hypoxia in response to treatment, Cell Death Discov 9 (2023) 1–8, https://doi.org/10.1038/s41420-023-01334-z.

[35] M. Geyer, L.-M. Gaul, S.L. D Agosto, V. Corbo, K. Queiroz, The tumor stroma influences immune cell distribution and recruitment in a PDAC-on-a-chip model, Front. Immunol. 14 (2023) 1155085, https://doi.org/10.3389/fimmu.2023.1155085.

[36] M.R. Haque, C.R. Wessel, D.D. Leary, C. Wang, A. Bhushan, F. Bishehsari, Patient-derived pancreatic cancer-on-a-chip recapitulates the tumor microenvironment, Microsyst Nanoeng 8 (2022) 1–13, https://doi.org/10.1038/s41378-022-00370-6.

[37] V. Sgarminato, S.L. Marasso, M. Cocuzza, G. Scordo, A. Ballesio, G. Ciardelli, et al., PDAC-on-chip for in vitro modeling of stromal and pancreatic cancer cell crosstalk, Biomater. Sci. 11 (2022) 208–224, https://doi.org/10.1039/D2BM00881E.

[38] D.-H.T. Nguyen, E. Lee, S. Alimperti, R.J. Norgard, A. Wong, J.J.-K. Lee, et al., A biomimetic pancreatic cancer on-chip reveals endothelial ablation via ALK7 signaling, Sci. Adv. 5 (2019), https://doi.org/10.1126/sciadv.aav6789 eaav6789.

[39] T. Song, H. Zhang, Z. Luo, L. Shang, Y. Zhao, Primary human pancreatic cancer cells cultivation in microfluidic hydrogel microcapsules for drug evaluation, Adv. Sci. 10 (2023) 2206004, https://doi.org/10.1002/advs.202206004.

[40] E. Driehuis, A. Gracanin, R.G.J. Vries, H. Clevers, S.F. Boj, Establishment of pancreatic organoids from normal tissue and tumors, STAR Protocols (2020), https://doi.org/10.1016/j.xpro.2020.100192.

[41] P. Tabeling, Introduction to Microfluidics, second ed., New to this Edition, Oxford University Press, Oxford, New York, 2023. Second Edition, New to this Edition.

[42] J.F. Dekkers, M. Alieva, L.M. Wellens, H.C.R. Ariese, P.R. Jamieson, A.M. Vonk, et al., High-resolution 3D imaging of fixed and cleared organoids, Nat. Protoc. (2019), https://doi.org/10.1038/s41596-019-0160-8.

[43] P. Bankhead, M.B. Loughrey, J.A. Fernández, Y. Dombrowski, D.G. McArt, P. D. Dunne, et al., QuPath: open source software for digital pathology image analysis, Sci. Rep. 7 (2017) 16878, https://doi.org/10.1038/s41598-017-17204-5.

[44] Barrier function readout analysis | emulate n.d. https://emulatebio.com/support/ep187-v1-0/. (Accessed 30 May 2024).

[45] L.A. Truman, C.A. Ford, M. Pasikowska, J.D. Pound, S.J. Wilkinson, I.E. Dumitriu, et al., CX3CL1/fractalkine is released from apoptotic lymphocytes to stimulate macrophage chemotaxis, Blood 112 (2008) 5026–5036, https://doi.org/10.1182/blood-2008-06-162404.

[46] D. Goldstein, R.H. El-Maraghi, P. Hammel, V. Heinemann, V. Kunzmann, J. Sastre, et al., nab-Paclitaxel plus gemcitabine for metastatic pancreatic cancer: long-term survival from a phase III trial, J Natl Cancer Inst 107 (2015) dju413, https://doi.org/10.1093/jnci/dju413.

[47] K.E. Poruk, M.A. Firpo, C.L. Scaife, D.G. Adler, L.L. Emerson, K.M. Boucher, et al., Serum osteopontin and tissue inhibitor of metalloproteinase 1 as diagnostic and prognostic biomarkers for pancreatic adenocarcinoma, Pancreas 42 (2013) 193–197, https://doi.org/10.1097/MPA.0b013e31825e354d.

[48] R.E. Brand, B.M. Nolen, H.J. Zeh, P.J. Allen, M.A. Eloubeidi, M. Goldberg, et al., Serum biomarker panels for the detection of pancreatic cancer, Clin. Cancer Res. 17 (2011) 805–816, https://doi.org/10.1158/1078-0432.CCR-10-0248.

[49] J. Song, L.J. Sokoll, J.J. Pasay, A.L. Rubin, H. Li, D.M. Bach, et al., Identification of serum biomarker panels for the early detection of pancreatic cancer. Cancer epidemiology, biomarkers & prevention : a publication of the American association for cancer research, Cosponsored by the American Society of Preventive Oncology 28 (2019) 174–182, https://doi.org/10.1158/1055-9965.EPI-18-0483.

[50] N. Martínez-Bosch, H. Cristóbal, M. Iglesias, M. Gironella, L. Barranco, L. Visa, et al., Soluble AXL is a novel blood marker for early detection of pancreatic ductal adenocarcinoma and differential diagnosis from chronic pancreatitis, EBioMedicine 75 (2022) 103797, https://doi.org/10.1016/j.ebiom.2021.103797.

[51] A.M. Kemas, R. Zandi Shafagh, N. Taebnia, M. Michel, L. Preiss, U. Hofmann, et al., Compound absorption in polymer devices impairs the translatability of preclinical safety assessments, Adv. Healthcare Mater. 13 (2024) 2303561, https://doi.org/10.1002/adhm.202303561.

[52] B.J. van Meer, H. de Vries, K.S.A. Firth, J. van Weerd, L.G.J. Tertoolen, H.B. J. Karperien, et al., Small molecule absorption by PDMS in the context of drug response bioassays, Biochem. Biophys. Res. Commun. 482 (2017) 323–328, https://doi.org/10.1016/j.bbrc.2016.11.062.

[53] The Organ-on-Chip Roadmap has been published. CEN-CENELEC n.d. https://www.cencenelec.eu/news-and-events/news/2024/brief-news/2024-07-10-organ-on-chip/(accessed September 7, 2024).
[54] C.F. Carlborg, T. Haraldsson, K. Öberg, M. Malkoch, W. van der Wijngaart, Beyond PDMS: off-stoichiometry thiol-ene (OSTE) based soft lithography for rapid prototyping of microfluidic devices, Lab Chip 11 (2011) 3136–3147, https://doi.org/10.1039/c1lc20388f.
[55] R. Geczy, D. Sticker, N. Bovet, U.O. Häfeli, J.P. Kutter, Chloroform compatible, thiol-ene based replica molded micro chemical devices as an alternative to glass microfluidic chips, Lab Chip 19 (2019) 798–806, https://doi.org/10.1039/c8lc01260a.
[56] A. Sontheimer-Phelps, B.A. Hassell, D.E. Ingber, Modelling cancer in microfluidic human organs-on-chips, Nat. Rev. Cancer 19 (2019) 65–81, https://doi.org/10.1038/s41568-018-0104-6.
[57] E.A. Aisenbrey, W.L. Murphy, Synthetic alternatives to Matrigel, Nat. Rev. Mater. 5 (2020) 539–551, https://doi.org/10.1038/s41578-020-0199-8.
[58] E.H. Nguyen, W.T. Daly, N.N.T. Le, M. Farnoodian, D.G. Belair, M.P. Schwartz, et al., Versatile synthetic alternatives to Matrigel for vascular toxicity screening and stem cell expansion, Nat. Biomed. Eng. 1 (2017) 96, https://doi.org/10.1038/s41551-017-0096.
[59] G.S. Offeddu, K. Haase, M.R. Gillrie, R. Li, O. Morozova, D. Hickman, et al., An on-chip model of protein paracellular and transcellular permeability in the microcirculation, Biomaterials 212 (2019) 115–125, https://doi.org/10.1016/j.biomaterials.2019.05.022.
[60] L. Claesson-Welsh, E. Dejana, D.M. McDonald, Permeability of the endothelial barrier: identifying and reconciling controversies, Trends Mol. Med. 27 (2021) 314–331, https://doi.org/10.1016/j.molmed.2020.11.006.
[61] P.D. Weinberg, Haemodynamic wall shear stress, endothelial permeability and atherosclerosis—a triad of controversy, Front. Bioeng. Biotechnol. 10 (2022), https://doi.org/10.3389/fbioe.2022.836680.
[62] Y.A. Komarova, K. Kruse, D. Mehta, A.B. Malik, Protein interactions at endothelial junctions and signaling mechanisms regulating endothelial permeability, Circ. Res. 120 (2017) 179–206, https://doi.org/10.1161/CIRCRESAHA.116.306534.
[63] J.M. Tarbell, Shear stress and the endothelial transport barrier, Cardiovasc. Res. 87 (2010) 320–330, https://doi.org/10.1093/cvr/cvq146.
[64] K. Corral-Nájera, G. Chauhan, S.O. Serna-Saldívar, S.O. Martínez-Chapa, M. M. Aeinehvand, Polymeric and biological membranes for organ-on-a-chip devices, Microsyst Nanoeng 9 (2023) 1–25, https://doi.org/10.1038/s41378-023-00579-z.
[65] L.C. Delon, Z. Guo, A. Oszmiana, C.-C. Chien, R. Gibson, C. Prestidge, et al., A systematic investigation of the effect of the fluid shear stress on Caco-2 cells towards the optimization of epithelial organ-on-chip models, Biomaterials 225 (2019) 119521, https://doi.org/10.1016/j.biomaterials.2019.119521.
[66] S. Fuchs, S. Johansson, A.Ø. Tjell, G. Werr, T. Mayr, M. Tenje, In-line analysis of organ-on-chip systems with sensors: integration, fabrication, challenges, and potential, ACS Biomater. Sci. Eng. 7 (2021) 2926–2948, https://doi.org/10.1021/acsbiomaterials.0c01110.
[67] J. Sabaté del Río, J. Ro, H. Yoon, T.-E. Park, Y.-K. Cho, Integrated technologies for continuous monitoring of organs-on-chips: current challenges and potential solutions, Biosens. Bioelectron. 224 (2023) 115057, https://doi.org/10.1016/j.bios.2022.115057.
[68] B.A. Krantz, E.M. O'Reilly, Biomarker-based therapy in pancreatic ductal adenocarcinoma: an emerging reality? Clin. Cancer Res. 24 (2018) 2241–2250, https://doi.org/10.1158/1078-0432.CCR-16-3169.
[69] L. Jiang, J. Qin, Y. Dai, S. Zhao, Q. Zhan, P. Cui, et al., Prospective observational study on biomarkers of response in pancreatic ductal adenocarcinoma, Nat Med 30 (2024) 749–761, https://doi.org/10.1038/s41591-023-02790-x.